Asian Journal of Chemistry; Vol. 31, No. 11 (2019), 2628-2634

ASIAN JOURNAL OF CHEMISTRY

https://doi.org/10.14233/ajchem.2019.22217

Isolation, Characterization, Molecular Docking and *in vitro* Studies of Inhibitory Effect on the Growth of Struvite Crystal Derived from *Melia dubia* Leaf Extract

G. Dayana Jeyaleela[1,*], J. Rosaline Vimala[1], R. Senthil[2,3], P. Anandagopu[2,3] and K. Manjula[4]

[1]PG and Research Department of Chemistry, Holy Cross College (Autonomous), Tiruchirappalli-620002, India
[2]Lysine Biotech Private Limited, Periyar Maniammai Institute of Science and Technology, Thanjavur-613403, India
[3]Faculty in Bioinformatics, Marudupandiyar Institutions, Thanjavur-613403, India
[4]Bio Techno Solutions Training and Research Institute, Tiruchirappalli-620020, India

*Corresponding author: E-mail: princedayana1221@gmail.com, dayana@hcctrichy.ac.in

Received: 27 May 2019; *Accepted*: 24 July 2019; *Published online*: 28 September 2019; AJC-19598

Present work aimed to isolate bioactive principle and its inhibitory potential against struvite stone by single diffusion method as well as docking studies to determine the mode of interaction between the complex structure of urease and rutin. Flavonoid compound is isolated from *Melia dubia* leaf extract with the help of TLC and column chromatography, and then characterized by ^{1}H & ^{13}C NMR, and LC-MS. Inhibitory potential of isolated flavonoid against kidney stone (struvite) is confirmed by molecular docking approach. Rutin acts as a urease inhibitor and the residues of urease namely 463Asp and 466 Ala were found to bind with rutin through hydrogen bonding and van der Waals interactions. *In vitro* study, the results revealed that with an increase in concentration of flavonoid rutin (1-5 mg/mL) the weight of the harvested crystals were gradually reduced from 2.8 cm to 0.5 cm and weight 0.662 g to 0.322 g at 5 mg/mL concentration. The XRD result of C+5 shows well inhibition on struvite crystal in all the planes and in SEM analysis, rutin inhibited crystal, surface of the crystal was damaged, whereas control shows pure and no defects on it.

Keywords: *Melia dubia*, Rutin, Struvite stone, Molecular Docking, Single diffusion method.

INTRODUCTION

Kidney or urinary stone (urolithiasis), is formed by crystal aggregation in the kidneys *via* dietary minerals in the urine. [1,2]. About 20 % of human population is affected by urolithiasis and is formed by a multi-process which is interconnected to diet, urinary tract infection, decreased urinary drainage, and microliths, *etc*. Most of the urinary stones are composed of phosphates, oxalates, cystine and uric acid [3]. Among all the phosphates stones, struvite (ammonium magnesium phosphate hexahydrate, $NH_4MgPO_4{\cdot}6H_2O$) and new berryite (magnesium hydrogen phosphate trihydrate, $MgHPO_4{\cdot}3H_2O$) are common constituents of urinary stones [4-6]. They occur in both adults and children [7]. In humans, struvite stones are formed as a result of urinary tract infection, when the urea-splitting urolithic organisms infect the urinary tract, bacteria segregate the urea excreted in urine in the presence of urease enzyme. It accelerates the formation of ammonia in urine and rendering it alkaline. In an alkaline state, supersaturated urine leads to nucleation, crystal growth and aggregation [8] thus, reduces the solubility of ammonium magnesium phosphate and leads to formation and deposition of struvite crystals [9]. Urea-splitting urolithic microorganisms, *Proteus*, *Pseudomonas*, *Mycoplasma*, *Klebsiella*, *Staphylococcus*, and yeast can hydrolyze urea to ammonia and raise the alkaline nature (pH) of urine [10,11]. Infection stones, urease, triple-phosphate stones and magnesium ammonium phosphate stone are the common names of struvite stone. About 10-15 % of urinary calculi consist of struvite stones and no clinical treatment is available to dissolve the stones already formed in the kidney, except for diuretics that flush out the stones through urinary tracts [12].

Plant-based compounds are safe and have less or no side effects on the treatment of any diseases compared to commercial drugs. Traditionally, herbal extracts and medicinal plants were used to prevent and treat the kidney stones. But, their exact mechanism in the inhibition of struvite due to the lead

bioactive principles is still unknown. Furthermore, molecular docking on struvite crystal was studied by only a few chemically synthesized compounds like β-mercaptoethanol, citrate and aluminum [13], *etc*. Thus, this research was aimed to study the inhibition potential of rutin flavonoid isolated from *Melia dubia* leaf on struvite stone by *in vitro* analysis along with molecular docking studies. To understand the mode of interaction of the complex of urease (struvite) with rutin and also seeking directions in space and conformations favourable for rutin binding to a urease.

EXPERIMENTAL

The chemicals sodium metasilicate (SMS), ammonium dihydrogen phosphate, magnesium acetate and methanol used in the assay are standardized brand and purchased from Eswarre Scientific Chemicals, Tiruchirappalli, India. Bio-Inhibitor used in the study was rutin which is isolated and characterized by *Melia dubia* leaves.

Extraction, isolation and separation of bioactive principle from *Melia dubia*: A dry powdered form of *Melia dubia* leaves (500 g) were extracted with hexane followed by chloroform to remove the chlorophylls and low polar impurities. The remaining residual plant material was further extracted with methanol by Soxhlet extraction method and concentrated by rotary evaporator. Concentrated methanol extract is subjected to TLC and column for isolation process and the final fraction is purified by preparative HPLC.

Characterization of flavonoid: Isolated compound was identified as flavonoid from the phytochemical screening test and further characterized with the help of spectral techniques such as UV-visible, FT-IR, ^{1}H & ^{13}C NMR and LC-MS [14-16].

Molecular docking studies on struvite binding with rutin

Preparation of the model for docking: The struvite protein urease downloaded from the database (PDB ID-1UBP) was co-crystallized with the inhibitor β-mercaptoethanol. The 3D structure of urease was obtained by X-ray diffraction with a resolution 1.65 Å. Downloaded urease was crystallized as a trimer of three A, B, C monomer chains, each monomer consisting of 6041 atoms and more than 25 heteroatoms as an inhibitor. Initially, C chain was chosen for the interaction and it is prepared by removing water molecules, small molecules and the two chains A and B from the trimer. The resulted C chain has the amino acids forming the active sites with the aim mainly to study the mode of interactions between the enzyme urease and rutin inhibitor (polyatomic) [13].

Before the interaction study, the Swiss Dock server was used to identify clusters and potential targets. With the cluster details, protein and ligand properties have been prepared by molecular graphics laboratory tools (MGL-1.5.6 version, Scripps Research Institute, Florida, FL, USA). Complex structures were modeled using modeling software's Pymol (1.1 version, Delano Scientific LLC, San Carlos, CA, USA), Chimera (1.10.1 version UCSF Resources for biocomputing visualization and informatics, NIH, USA) and Ligplot (1.4.5. version, European Bioinformatics Institute,Cambridge CB10 1SD, UK) [17,18].

***in-vitro* Analysis of struvite stone by single diffusion gel method:** The inhibitory potential of rutin on the growth of struvite stone was carried out by adopting a single diffusion gel method. A gel was prepared by mixing known volume of sodium metasilicate of specific gravity 1.03 g/cc with diammonium hydrogen orthophosphate of 7.7 pH and it acts as a growth medium to provide the simplified model for complexation of urinary calculi. Rutin was dissolved in methanol and made into various concentrations such as 1, 2, 3, 4 & 5 mg/ml. After gelation 2M solution of magnesium acetate was added in different ratio with rutin. The control crystal (without inhibitor rutin) was grown by adding 15 mL of magnesium acetate gently poured on the gel. Meanwhile, negative control *viz*. water and methanol were mixed, 5 mL of each with 10 mL of magnesium acetate separately in a separate boiling test tubes containing the gel. In the case of rutin addition, different concentrations of 5ml rutin were pipetted out and added along with 10 mL of magnesium acetate solution in the rest of the tubes (C+1, C+2, C+3, C+4 and C+ 5). After pouring the supernatant solution in the respective tubes, all the test tubes were capped tightly with air-tight stoppers [19]. The full experiment was carried out in an aseptic condition at room temperature and kept in a laminar airflow chamber to avoid microbial contamination. The reaction shown below was expected to happen in the gel between the reactants:

$$NH_4H_2PO_4{\cdot}2H_2O + (CH_3COO)_2Mg{\cdot}4H_2O \longrightarrow NH_4MgPO_4{\cdot}6H_2O + 2CH_3COOH$$

Grown crystals were harvested by decanting whole content from boiling test tube and the gel could be removed by dissolving in water [20].

Characterization of struvite crystal: Growth features of formed magnesium ammonium phosphate *i.e*. struvite crystal (MAP) were asserted by spectral and physical techniques. Size and weight of MAP crystal in control and treated were measured with the help of a scale and weighing balance. A small portion of the crystals grown from non-treated and treated was taken for the FT-IR analysis to identify the functional groups and their shifts in not inhibited and inhibited MAP. Few mg of crystals were well ground with spectroscopic grade KBr pellets. The MAP crystals were washed with water, air-dried and mounted on aluminium stubs using carbon tape further sputtered with gold to study the surface analysis at low and high magnifications with the help of SEM. MAP obtained in above conditions were crushed and made it into powder to examine the crystalline phase of the crystals by XRD analysis under Cu-Kα with λ = 1.54056 Å, Ni filter of Bragg's angles $20^{\circ} < 2\theta < 70^{\circ}$ at room temperature [21].

RESULTS AND DISCUSSION

UV-visible and FT-IR analysis: An absorption spectrum of isolated flavonoid compound was observed at 256 nm (band-II) for ring A and 355 nm (band-1) for ring B in the flavonoid nucleus (Fig. 1). In FT-IR spectra, a peak at 3365 cm^{-1} gives strong evidence for the presence of free OH group in the isolated flavonoid compound and a peak at 1612.49 cm^{-1} responsible for C=O in flavonoid nucleus (Fig. 2).

NMR analysis: Proton NMR spectra of isolated flavonoid compound gives peak at δ 12.602 responsible for OH proton in C5 (singlet) similarly 6.196 and 6.191 (d, 1H in C6), 10.831 (s, OH in C7), 6.387 and 6.382 (d, 1H in C8), 7.530 (dd, 1H in C2′), 9.182 (s, OH in C3′), 9.672 (s, OH in C4′), 6.849 and 6.829

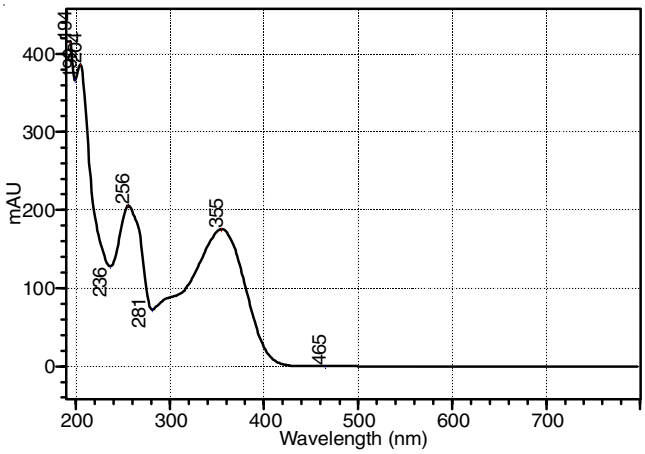

Fig. 1. UV-visible spectrum of isolated flavonoid

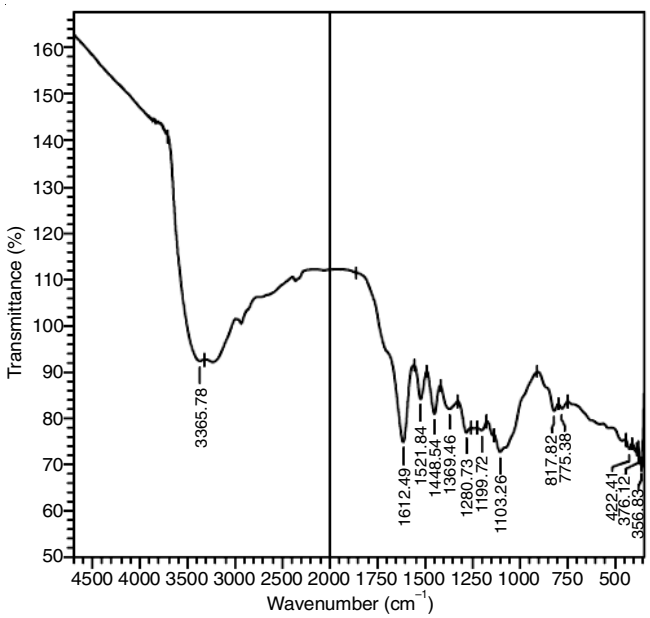

Fig. 2. FT-IR spectrum of isolated flavonoid

(dd, 1H in C5′), 7.549 (dd, 1H in C6′), peak at 2.3 represents DMSO solvent peak and multi-peak between 3 to 6 ppm responsible for glycosides linkage in flavonoid nucleus. For G ring, peaks at 5.353 and 5.335 (dd, 1H in C1′), 4.414 and 4.379 (dd, H & OH in C2′), 3.717 (td) and 3.692 (dt) (H & OH in C3′), peat at 3.093 (dd) to 3.047(dd) (H & OH in C4′), 3.308 (td, C5′), 3.293 and 3.271 (dd, 2H, in C6′), for the ring H peak at 3.382 and 3.355 (d, 1H in C1′), 3.217 and 3.207 (dd, H & OH in C2′), peak at 3.250 (td) to 3.2225 (t) (H & OH in C3′), peak at 2.507 to 2.499 (dd, H & OH in C4′), 3.263 (qd, 1H in C5′), 1.070 and 1.055 (d, 3H in C6‴).

In case of ^{13}C spectra, solvent peak obtained at 40 ppm and a peak at 156.853 responsible for C2 carbon in the same manner 133.740 (C3), 177.804 (C4), 157.039 (C5), 99.5 (C6), 164.490 (C7), 94.014 (C8), 161.655 (C9), 104.408 (C10), 122.021 (C1′), 115.654 (C2′), 145.188 (C3′), 148.844 (C4′), 116.700 (C5′), 121.611 (C6′), for the G ring 101.186 (C1′), 74.503 (C2′), 70.994 (C3′), 72.272 (C4′), 76.346 (C5′), 67.423 (C6′), for the H ring 70.808 (C2′), 70.994 (C3′), 70.436 (C4′). 68.678 (C5′), 18.177 (C6′) .

LC-MS of isolated flavonoid rutin: Mass spectrum and its fragmentations of isolated flavonoid rutin are shown in Figs. 3 and 4. The fragmentation with their collision energy of the isolated compound is shown in Table-1. It clearly explains the major parent molecular ion (M+1) peak at *m/z* = 611.16 responsible for flavone-3-rutinoside, 3,3′,4′,5,7-pentahydroxy (rutin). Based on MSMS fragments obtained from *m/z* 611[+ve], the proposed fragmentation pathway of compound is displayed in Fig. 4. From the above shreds of evidence, the molecular formula of isolated flavonoid compound is $C_{27}H_{30}O_{16}$ and the accurate molecular weight is found to be 610.5175.

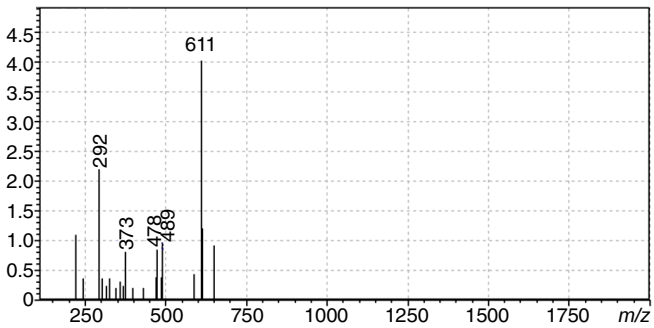

Fig. 3. LC-MS result of isolated flavonoid rutin

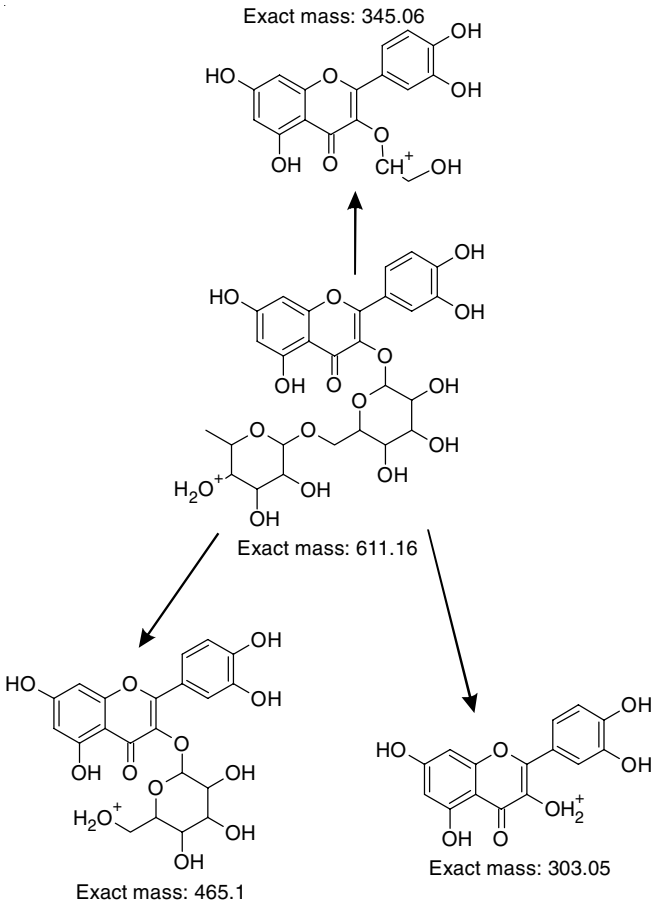

Fig. 4. Possible mass fragmentation of flavone-3-rutinoside, 3,3',4',5,7-pentahydroxy

Molecular docking on struvite stone: The binding ability of rutin with urease receptor using molecular modeling tools was carried out and Fig. 5 represents the 3D structure of trimer of urease. Fig. 6 represents the monomer of side chain-C in urease, while Fig. 7 indicates the ball and stick representation

TABLE-1
MSMS DATA OF *m/z* 611(+ve) UNDER DIFFERENT COLLISION ENERGIES USING ESI POSITIVE IONIZATION

Collision energy	MS-MS Fragmentation of *m/z* 611 (+VE)					
-5	611	465	345	303		
-10	611	465	345	303		
-15	611	465	345	303		
-25		464	345	303	85	
-35				303	85	71
-45				303	85	71
-55			345	303	85	71
-60				303	85	71

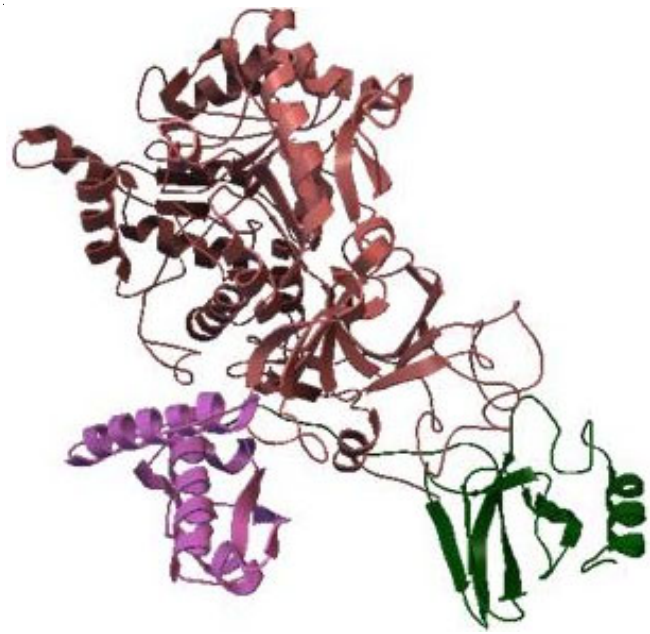

Fig. 5. 3D structure of trimer of urease

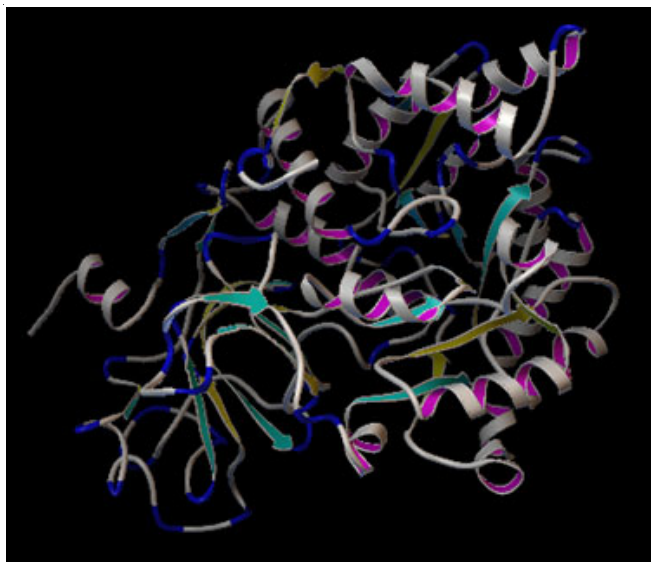

Fig. 6. 3D representation of monomer-side chain (C)

of ligand rutin. Molecular docking algorithm executed, provides information related to best fit through the cluster, ranking and affinity values. With an affinity score/energy -8.1721735 Kcal/mol, the receptor-ligand structure modeled for interaction studies.

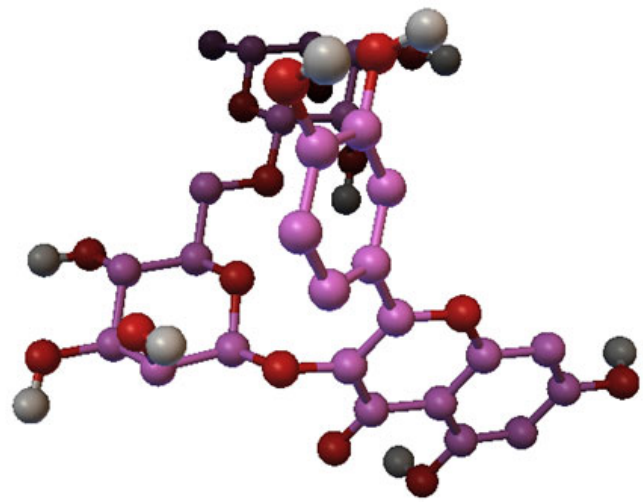

Fig. 7. Structure of rutin

The complex structure of rutin binding with urease is shown in Fig. 8. Fig. 9 represents the schematic diagram of interactions of rutin along with urease and it manifests the rutin interaction with different amino acids of urease by hydrogen and hydrophobic bonding. Amino acid residues Asp 463 and Ala 466 form the hydrogen bond between the receptor (urease) and ligand (rutin) with a radius of 2.78 and 3.17 Å, respectively, denoted by green dashed lines. Residues subsequently made hydrophobic interactions with ligand through non-bonded method are Ile 468, Pro 469, Ile 461, Tyr 410, Met 475 and Pro 464, indicated by black dotted lines.

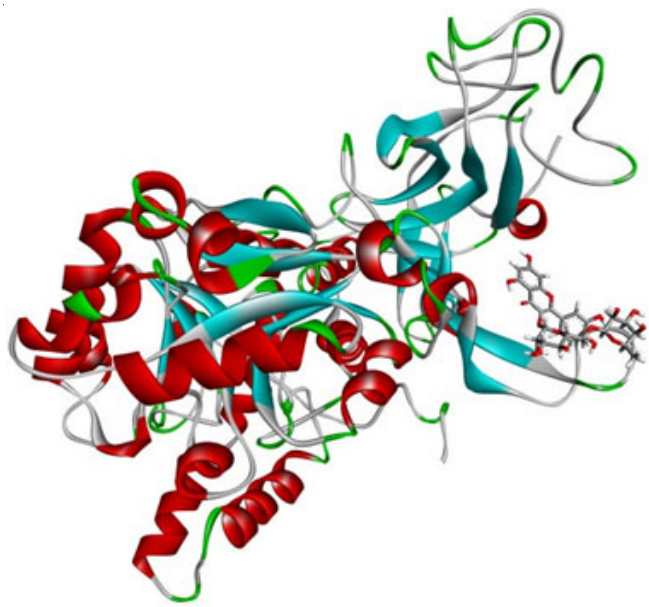

Fig. 8. Images of rutin binding with urease

Size and yield of harvested struvite crystals: Urinary calculi growth depends on the constant supplement of required nutrients in the urinary system since that dissolution or inhibition of these nutrients to be achieved; adding potential extract or compounds to the nutrients is one of the ways to control the MAP crystal growth. The MAP crystals are usually found in different morphologies such as star type, coffin shape, feather-shaped dendritic, needle type, a prismatic shape, pyramidal

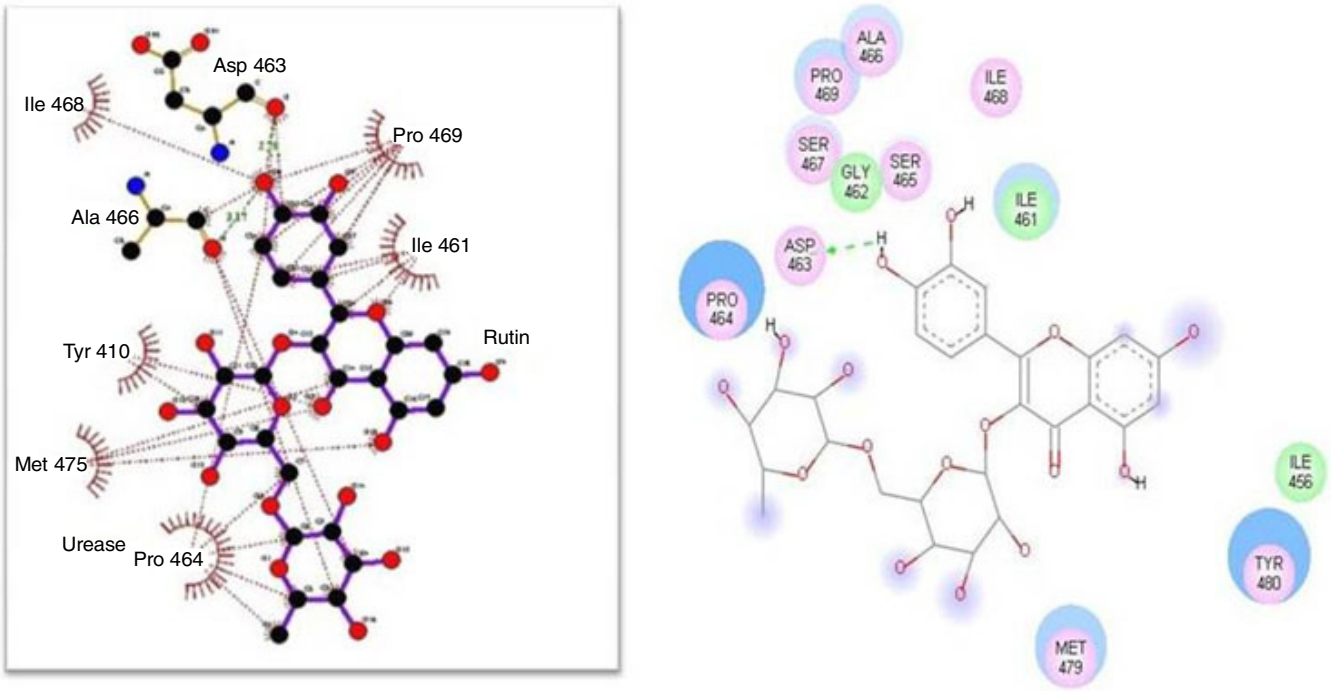

Fig. 9. Mode of interactions of rutin binding with urease

type, rectangular platelet type, X shaped dendritic and Y shaped dendritic [21]. In C, C+W and C+M commonly feather shaped dendritic and star type crystals were appeared at nucleation, whereas in the rutin additions (C+1 to C+5) X shaped dendritic, Y shaped dendritic crystals and star type was developed in depth of gel. Meanwhile, nucleation is arrested because of rutin retard the growth process of struvite crystals. The result of size and weight of the crystals obtained in treated and non-treated MAP are shown in Table-2. It is found that in control, C+W and C+M, the size of crystal is more or less similar *i.e*. 1.7 cm, 1.42 cm, 1.53 cm, respectively. On the other hand in case of the rutin additive crystals, they gradually showed well inhibition on the growth of struvite. At higher concentration, 5 mg/mL *i.e*. C+5 showed the great inhibition and size of the crystal reduced to 0.38 cm. Similarly, the weight of crystal on the treatment with control is 0.662 g and well-treated C+5 is 0.280 g. Thus, on treatment with rutin, the growth of struvite crystal is delayed same time retards. Two types of mechanism is possible for the dissolution of MAP crystals, rutin forming stable complex with Mg^{2+} *i.e*. urinary nutrient and thus disrupt constant supplement of Mg^{2+} ions for the growth of MAP, or by adsorbing or doping rutin on the MAP crystal surface and thus leads to weakening of MAP crystal bonds and resulting fragmentation of MAP is possible.

TABLE-2
ANOVA STATISTICAL ANALYSIS FOR WEIGHT AND SIZE OF THE MAP CRYSTALS OBTAINED BY CONTROL AND RUTIN TREATED

Sample name	Weight of crystals (g)	Size of crystals (cm) ± SD
Control (C)	0.662±0.0113	1.72±0.0085
Control + Water (C+W)	0.495±0.0256	1.42±0.0017
Control + Methanol (C+M)	0.404±0.0620	1.53±0.0052
Control + 1 mg/mL of rutin (C+1)	0.365±0.0318	1.15±0.0470
Control + 2 mg/mL of rutin (C+2)	0.343±0.0020	1.06±0.0198
Control + 3 mg/mL of rutin (C+3)	0.322±0.0402	0.85±0.0735
Control + 4 mg/mL of rutin (C+4)	0.301±0.0109	0.60±0.0003
Control + 5 mg/mL of rutin (C+5)	0.280±0.0056	0.38±0.0028

FT-IR analysis: Literature reveals that the struvite is an orthorhombic system consisting of three functional groups namely PO_4, $Mg{\cdot}6H_2O$ and NH_4 groups and all are held together by hydrogen bonding [22]. Thus, the peaks between 3550 and 3280 cm^{-1} is due to OH stretching vibrations of water. The peaks at 3000-2800 and 1750-1630 cm^{-1} is responsible for the N-H symmetric stretching, symmetric and asymmetric bending vibrations of NH_4 units, respectively. Frequency ranging at 995-930 and 1163-1017 cm^{-1} are due to symmetric vibrations of PO_4 units. Similarly, the peaks appearing at 470-404 and 554-509 cm^{-1} are responsible for bending vibration and asymmetric bending modes of PO_4 units, respectively. Magnesium and oxygen bond vibration and deformations are found at 650-400 and 847 cm^{-1}. The peak appearing in the control and intreated crystal shows the functionality of NH_4, $Mg{\cdot}6H_2O$, and PO_4 which all abide with library data. In comparison, no significant shift or change in their frequency is seen for C, C+W and C+M, whereas significant shifts in the frequencies of functional groups are clearly noticed in the crystal treated with rutin of different concentration C+1, C+2, C+3, C+4 and C+5 and the results are shown in Fig. 10. The inhibition starts from even at 1 mg/mL concentration of rutin and it shows the same trends on increasing its concentration towards struvite crystals. At 5 mg/mL concentration the inhibition is very high and the size of the crystal becomes tiny than the control. The well-inhibited (5 mg/mL C+5) and control crystal were further taken for SEM and XRD analysis to study the effects of rutin on struvite.

XRD analysis of control and C+ 5 crystals: Fig. 11 shows the powdered XRD report of C and C+5 crystals with the assigned planes indicated therein. The lattice constant a = 6.954 Å, b = 6.140 Å, c = 11.216 Å with interfacial angle $\alpha = \beta = \gamma = 90^{\circ}$

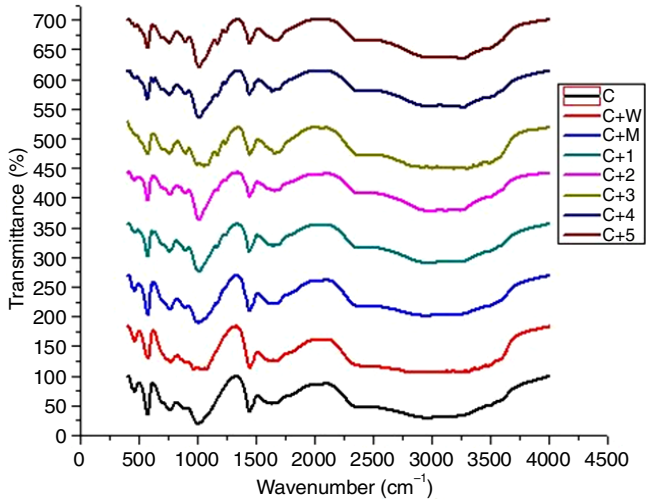

Fig. 10. Combined FT-IR graph of control and rutin treated MAP: (C) Control MAP, (C+W) Water additive MAP, (C+M) Methanol additive MAP, (C+1) 1 mg/mL rutin additive MAP, (C+2) 2 mg/mL rutin additive MAP (C+3) 3 mg/mL rutin additive MAP (C+4) 4 mg/mL rutin additive MAP (C+5) 5 mg/mL rutin additive MAP

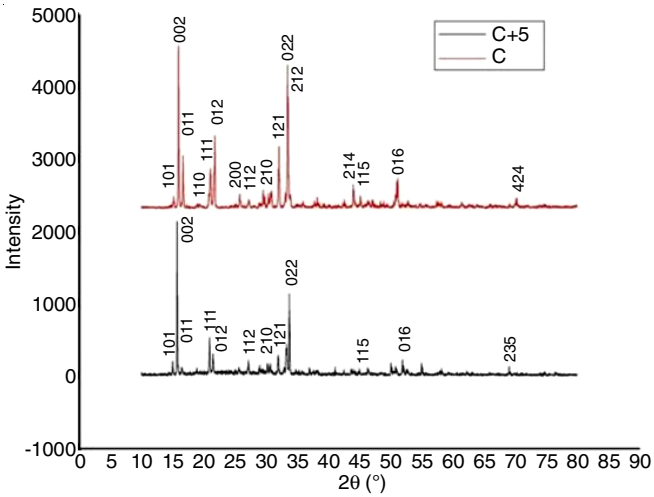

Fig. 11. XRD results of C and C+5 MAP crystals

shows that the formed struvite belongs to orthorhombic crystal structure. XRD result of C+5 agree with the decrease in the intensity of all the plane intensity of MAP after adding rutin and it evidenced rutin suppress the growth of struvite crystals *i.e*. C+5 shows very good inhibition on struvite crystal in all the planes except 002 planes.

SEM analysis of struvite crystal: Morphological study of control (C) and well-inhibited MAP crystals (C+5) were studied and their surface images are shown in Fig. 12. The surface of pure crystal *i.e*. control MAP appeared clean and free from major defects but in rutin treated crystal the surface of crystal was damaged and due to doping of rutin on the surface of crystal is found.

Conclusion

The study summaries that the biologically active flavonoid is successfully isolated from *Melia dubia* leaf by combined chromatography methods. From the molecular docking, the binding potential of rutin towards struvite stone is achieved. The experimental data *in vitro* evidenced the docking results and dissolution rate of MAP crystals is increased with an increase in the concentration of rutin. Even at low concentration (1 mg/mL rutin) the nucleation is disrupted and delayed. Maximum dimension or length of the urinary crystal was reduced to smaller size and smaller dimension which can easily pass through the urinary tract. The dissolution rate of struvite crystals is enhanced while adding rutin to the urinary nutrients.

ACKNOWLEDGEMENTS

One of the authors, J. Rosaline Vimala extends her appreciation to the University Grants Commission (UGC), Hyderabad, India, for funding the work through the minor research project No. F MRP-5665/15 (SERO/UGC).

CONFLICT OF INTEREST

The authors declare that there is no conflict of interests regarding the publication of this article.

REFERENCES

1. R. Flannigan, W.H. Choy, B. Chew and D. Lange, *Nat. Rev. Urol.*, **11**, 333 (2014); https://doi.org/10.1038/nrurol.2014.99.

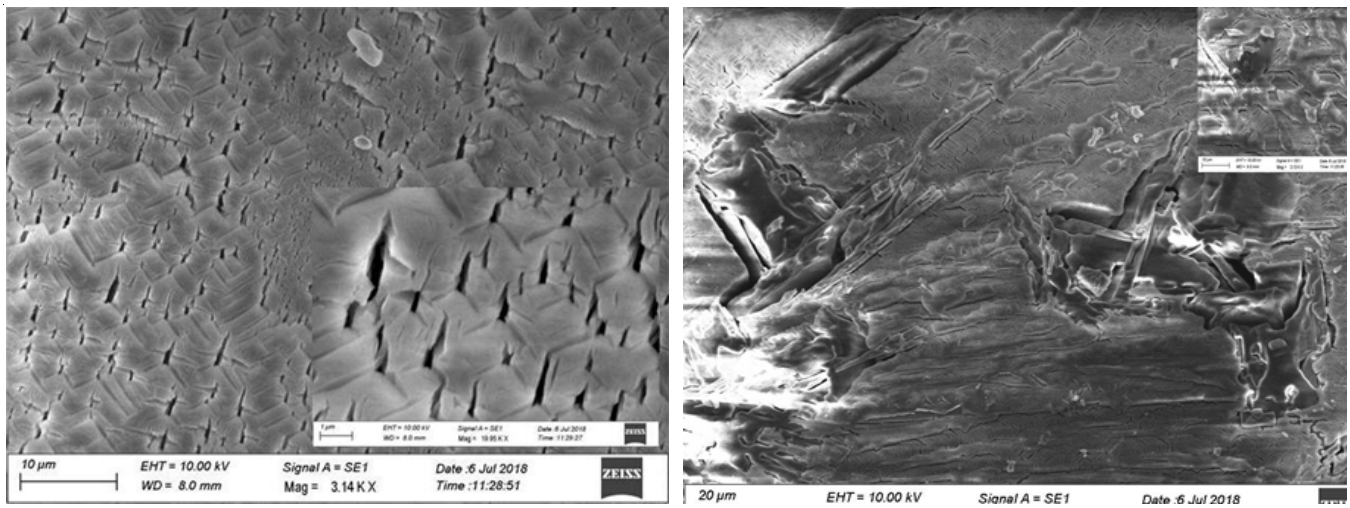

Fig. 12. SEM results of the control MAP crystal and well inhibited (C+5) MAP crystal

2. L. Benramdane, M. Bouatia, M.O.B. Idrissi and M. Draoui, *Spectrosc. Lett.*, **41**, 72 (2008); https://doi.org/10.1080/00387010801943806.
3. V. Butterweck and S.R.X. Khan, *Planta Med.*, **75**, 1095 (2009); https://doi.org/10.1055/s-0029-1185719.
4. P. Das, G. Gupta, V. Velu, R. Awasthi, K. Dua and H. Malipeddi, *Biomed. Pharmacother.*, **96**, 361 (2017); https://doi.org/10.1016/j.biopha.2017.10.015.
5. G. Mandel and N. Mandel, eds.: F.L. Coe, M.J. Favus, C.Y.C. Pak, J.H. Parks and G.M. Preminger, Analysis of Stones, In: Kidney Stones, Medical and Surgical Management, Lippincott-Raven: Philadelphiapp. 323-335 (1986).
6. F. Deng and J.M. Ouyang, *Mater. Sci. Eng. C*, **26**, 688 (2006); https://doi.org/10.1016/j.msec.2005.06.061.
7. M.A.P. Manzoor, B. Singh, A.K. Agrawal, A.B. Arun, M. Mujeeburahiman and P.-D. Rekha, *PLoS One*, **13**, e0202306 (2018); https://doi.org/10.1371/journal.pone.0202306.
8. M. Biocic, M. Saraga, A. Cvitkovic Kuzmic, Z. Bahtijarevic, D. Budimir, J. Todoric and R.M. Ujevic, *Coll. Antropol.*, **27**, 745 (2003).
9. H. Kuvezdic, A. Tucak, N. Peric, D. Prlic, I. Zoric and R. Galic, *Coll. Antropol.*, **27**, 71 (2003).
10. K.H. Bichler, E. Eipper, K. Naber, V. Braun, R. Zimmermann and S. Lahme, *Int. J. Antimicrob. Agents*, **19**, 488 (2002); https://doi.org/10.1016/S0924-8579(02)00088-2.
11. S. Muryanto, S. Sutanti and M. Kasmiyatun, Inhibition of Struvite Crystal Growth in the Presence of Herbal Extract *orthosiphon aristatus* BL.MIQ. MATEC web of conferences, 01013, pp. 1-5 (2016).
12. A. Torzewska and A. Rozalski, *Microbiol. Res.*, **169**, 579 (2014); https://doi.org/10.1016/j.micres.2013.09.020.
13. M. Beghalia, H. Allali, S. Ghalem, A. Belouatek and A. Sari, *Adv. J. Mol. Imaging*, **1**, 33 (2011); https://doi.org/10.4236/ami.2011.13005.
14. G.D. Jeyaleela, N. Balasubramani and J.R. Vimala, *Asian J. Pharm. Clin. Res.*, **12**, 107 (2019); https://doi.org/10.22159/ajpcr.2019.v12i2.28384.
15. N. Raaman, Phytochemical Techniques, New India Publication Agency: New Delhi, pp. 275-286 (2006).
16. J.B. Harborne, A Guide to Modern Techniques of Plant Analysis, Kluwer Academic Publisher: USA, edn 2, pp. 75-77 (1998).
17. M.A.A. Abdullah, G.E.-D.A.A. Abuo-Rahma, E.-S.M.N. Abdelhafez, H.A. Hassan and R.M. Abd El-Baky, *Bioorg. Chem.*, **70**, 1 (2017); https://doi.org/10.1016/j.bioorg.2016.11.002.
18. A.A. Mohammed, *Afr. J. Microbiol. Res.*, **10**, 81 (2016).
19. K. Suguna, M. Thenmozhi and C. Sekar, *Bull. Mater. Sci.*, **35**, 701 (2012); https://doi.org/10.1007/s12034-012-0322-6.
20. J. Prywer and A. Torzewska, *Evid. Based Complement Alternat. Med.*, **2012**, Article ID 862794 (2012); https://doi.org/10.1155/2012/862794.
21. C.K. Chauhan and M.J. Joshi, *J. Cryst. Growth*, **362**, 330 (2013); https://doi.org/10.1016/j.jcrysgro.2011.11.008.
22. M. Das, H. Malipeddi, N.A. Nambiraj and R. Rajan, *J. Food Biochem.*, **40**, 148 (2016); https://doi.org/10.1111/jfbc.12205.